Activity and Stability of Cu−CeO_2 Catalysts in High-Temperature Water−Gas Shift for Fuel-Cell Applications

Xiaomei Qi and Maria Flytzani-Stephanopoulos*

Department of Chemical and Biological Engineering, Tufts University, Medford, Massachusetts 02155

Copper-containing cerium oxide materials are shown in this work to be suitable for the high-temperature water−gas shift (WGS) reaction integrated with hydrogen separation in a membrane reactor to generate pure hydrogen. Copper−ceria is a stable high-temperature shift catalyst, unlike iron−chrome catalysts that deactivate severely in CO_2-rich gases. Such gas mixtures will prevail if a catalytic membrane reactor is used to remove hydrogen. We also found that iron oxide−ceria catalysts have much lower activities than copper−ceria catalysts. Ceria participates in the WGS reaction; its surface properties are crucial for high activity and are sensitive to the presence of dopants. The kinetics of the WGS reaction over 10 atom % Cu−Ce(30 atom % La)O_x were measured in the temperature range 300−450 °C. A strong dependence on CO and a weak dependence on H_2O were found at 450 °C, whereas inhibition by the reaction products was weak. The apparent activation energy over the catalyst stabilized in the reaction gas mixture at 450 °C is 70 kJ/mol. The catalyst lost some activity in the initial time on stream but was stabilized thereafter. A loss of catalyst surface area (∼20%) and copper enrichment of the ceria surface during the WGS reaction at 450 °C can explain the observed activity loss.

Introduction

The exothermic water−gas shift (WGS) reaction, CO + H_2O ↔ CO_2 + H_2, is used industrially for the production of hydrogen for use in ammonia synthesis and in adjusting the CO/H_2 ratio for subsequent synthesis of methanol. Recently, there has been a renewed interest in the WGS reaction because of its potential use in supplying hydrogen for fuel-cell power generation. Fuel cells are currently undergoing rapid development for both stationary and transportation applications.

Industrially, the WGS reaction is carried out in two temperature regimes: High-temperature (320−450 °C) shift reactors use an Fe_2O_3−Cr_2O_3 catalyst[1,2] that can effectively reduce CO from several percentage points to the equilibrium CO value dictated by the operating temperature and composition; further reduction of CO takes place at low temperatures over a more active catalyst based on Cu−ZnO.[1,3] Another industrially applied catalyst is Co−Mo/Al_2O_3 (used in the 150−400 °C temperature range), which is sulfur-tolerant.[1,4] The Cu−ZnO catalyst is very sensitive to temperature excursions, operating in the narrow temperature window of 200−250 °C; requires careful activation in H_2 gas; and is readily deactivated by exposure to air or by water condensation.

Optimization of the WGS system for the production of hydrogen for fuel cells is of particular interest to the energy industry. The high-temperature shift (HTS) can be used to increase the hydrogen content of coal gas produced by gasification or of reformate gas produced by autothermal reforming of fuel oils. To this end, it is desirable to couple the WGS reaction to hydrogen separation using a semipermeable membrane, with both processes taking place at high temperatures to improve the reaction kinetics and permeation.[5] Reduced equilibrium conversion of CO at high temperatures is overcome by product H_2 removal via the membrane. There are several challenges in developing a HTS membrane reactor that is small and cost-effective. If Pd-based, the membrane should contain a minimal amount of Pd, and the catalyst should be both robust and active in CO_2-rich gas. This type gas will be present over much of the catalyst, as the membrane removes the hydrogen produced from the water−gas shift reaction.

Commercial catalyst formulations containing iron oxide were recently found to deactivate in CO_2-rich gases.[6] In this work, we examine Cu-containing ceria catalysts as an alternative to the commercial iron−chrome HTS catalysts. For comparison, we also prepared and studied iron oxide-containing ceria catalysts.

CeO_2-based catalysts have been found promising for the WGS reaction.[7−14] When treated in a reducing atmosphere (such as CO, H_2, and hydrocarbons) at elevated temperatures, CeO_2 forms a continuum of oxygen-deficient, nonstoichiometric oxides, CeO_{2-x} ($0 < x \leq 0.5$),[15] that can be reoxidized to CeO_2 when exposed to an oxidizing environment (such as oxygen, water vapor, or NO). CeO_2 retains its fluorite-type crystal structure even after the loss of considerable amounts of oxygen and the formation of a large number of oxygen vacancies. Doping of ceria with ZrO_2 or La_2O_3 increases its reducibility, oxygen storage capacity, and resistance to sintering.[16,17] Noble metals (Rh, Pt, Pd)[7,8] and non-noble metals (Au, Cu)[9−14] on CeO_2 have been reported as promising low-temperature WGS catalysts. Bunluesin et al.[7] found that Pt, Pd, and Rh supported on ceria had specific WGS reaction rates (normalized to the catalyst area) identical for each of the metals and much higher than those for either pure ceria or each of the precious metals supported on alumina. They proposed that the water−gas shift on ceria-supported precious metals occurs through a bifunctional redox mechanism in which CO adsorbed on the precious metal is oxidized by ceria, which, in turn, is oxidized by water. Rivaling the precious metal−ceria catalysts is the Au−ceria system, which was recently reported as both very active

* To whom correspondence should be addressed. Tel.: 1-617-627-3048. Fax: 1-617-627-3991. E-mail: mflytzan@tufts.edu.

10.1021/ie0306170 CCC: $27.50
Published on Web 03/26/2004

and stable in the WGS reaction at temperatures in the range of 175−350 °C and in realistic feed gas compositions.[9−11]

Li et al.[13] recently reported on the WGS activity of Cu- and Ni-containing ceria catalysts over the temperature range of 175−300 °C. The catalysts were prepared by the urea gelation coprecipitation method, which disperses the metal/metal oxide in the form of clusters on ceria, resulting in a large interfacial area and interaction with the reducible cerium oxide support. The content of Cu or Ni was in the range of 5−15 atom % (2−8 wt %), and 10 atom % La_2O_3 was doped into ceria as a structural stabilizer. The 5% Cu−Ce(La)O_x catalyst was reported to retain high activity and stability at temperatures up to 600 °C.[13] However, the gas used in that work comprised only CO and H_2O. It is important to examine the stability of such catalysts in the presence of realistic reformate gas compositions. Such gases were used in a recent kinetic study of Cu-based shift catalysts, including copper−ceria, but only at ∼200 °C.[14] The high-temperature stability of such catalysts needs to be evaluated.

The choice of copper−ceria for HTS applications is further rationalized by the following consideration: The formulation contains a nonprecious metal; hence, it would be a much more cost-effective catalyst for the intended application. It is also a better choice than nickel−ceria, which catalyzes the methanation reaction,[12] and it has better activity than gold−ceria at high temperatures.[12] Several groups have reported that the addition of a small amount of CeO_2 into the Fe_2O_3−Cr_2O_3 catalyst or Cr-free Fe_2O_3 catalyst enhances the performance of the catalyst.[18−20] To examine whether iron oxide supported on ceria has as good activity as the copper−ceria system, Fe−Ce(La)O_x was also studied in this work.

Experimental Section

Catalyst Preparation. Cu- or Fe-containing ceria catalysts were prepared by the urea gelation coprecipitation (UGC) method,[13] which produces more homogeneous mixed oxides with finer particle sizes than conventional coprecipitation. The UGC method consists of the following steps: (1) Dissolve urea; $(NH_4)_2Ce(NO_3)_6$, $La(NO_3)_3$, or $ZrO(NO_3)_2$; and $Cu(NO_3)_2{\cdot}3H_2O$ or $Fe(NO_3)_3{\cdot}9H_2O$ in required amounts in deionized water. (2) Heat the solution to boiling, (3) adding water when precipitation begins (about 30 min after boiling). (4) Age the precipitate in boiling water with constant stirring and addition of water for 8 h. (5) Filter and wash the precipitate twice in 50−70 °C water with constant stirring for 30 min each time and (6) dry the precipitate at about 100 °C for 8 h. The dried lump was then crushed into particles smaller than 150 μm in diameter and calcined in air by being heated slowly (2 °C/min) to 650 °C and kept at this temperature for 4 h.

Several catalyst formulations were prepared with La_2O_3 or ZrO_2 used as a dopant in ceria in amounts ranging from 8 to 30 atom %. Dopants were added to improve the thermal stability of ceria.[16,17] Copper or iron oxide was added as a minor component in ceria. All compositions are expressed in atomic percentages. As an example, the notation 10% Cu−Ce(30% La)O_x means

$$\mathrm{Cu}/(\mathrm{Cu}+\mathrm{Ce}+\mathrm{La}) = 0.10$$

$$\mathrm{Ce}/(\mathrm{Cu}+\mathrm{Ce}+\mathrm{La}) = 0.90 \times 0.70$$

and

$$\mathrm{La}/(\mathrm{Cu}+\mathrm{Ce}+\mathrm{La}) = 0.90 \times 0.30$$

C12-4-02, a commercial catalyst containing 80−95 wt % Fe_2O_3, 5−10 wt % Cr_2O_3, <5 wt % CrO_3, 1−5 wt % CuO, and 1−5 wt % graphite, was supplied by United Catalysts, Inc., in pellet form and was used after being crushed into <150-μm-size particles.

Catalyst Characterization. The elemental composition of each sample was determined by inductively coupled plasma (ICP) spectrometry. Hydrogen peroxide and nitric acid were used to dissolve the solids at room temperature.

The BET surface area of each sample was measured by single-point nitrogen adsorption/desorption cycles in a Micromeritics Pulse Chemisorb 2705 instrument, using a 30% N_2/He gas mixture.

X-ray powder diffraction (XRD) analysis was performed on a Rigaku 300 X-ray diffractometer with rotating anode generators and a monochromatic detector. Cu K_α radiation was used. Samples in fine powder form were directly pressed onto a $^3/_4$-in. by $^5/_8$-in. frosted area etched on a glass holder. A small amount of tungsten powder was added to the sample to calibrate the peak position. The crystal size of ceria was determined by the Scherrer equation,[21] and the lattice constant of ceria was determined from Bragg's law.[21]

Temperature-programmed reduction (TPR) tests with H_2 were run in the same instrument according to the following procedure: A sample of about 1 g was heated to 350 °C (10 °C/min) in 50 mL/min (NTP) 20% O_2/He and kept at this temperature for 30 min to fully oxidize the sample. Heating was then stopped, and when the temperature dropped to 200 °C, purge gas, 50 mL/min N_2 (99.999%), was switched in. TPR began after the sample had cooled to room temperature. The reduction gas was 20% H_2/N_2 (50 mL/min), and the heating rate was 5 °C/min.

Temperature-programmed oxidation (TPO) tests were run according to the following procedure: The sample was heated to 350 °C (10 °C/min) in He (99.999%, 50 mL/min) and kept at 350 °C for 30 min to remove any CO_2 adsorbed. After the sample had cooled to room temperature, it was heated in a 20% O_2/He (50 mL/min) gas mixture to 650 °C at a heating rate of 5 °C/min. A mass spectrometer (MKS-model RS-1) was used for detection of CO_2.

X-ray photoelectron spectroscopy (XPS) was performed using a Perkin-Elmer 5200C instrument with a 300-W (15-kV by 20-mA) aluminum K_α anode as the X-ray source. Samples used in XPS analysis were in powder form pressed on a double-sided adhesive copper tape. The tape with the sample was mounted on a sample holder and introduced into the XPS vacuum chamber. Analysis was performed after a desired low pressure in the vacuum chamber had been reached.

Activity Tests in a Packed-Bed Microreactor. CO conversion tests and WGS reaction rate measurements were performed at atmospheric pressure. Catalyst samples (<150 μm in size) were diluted with quartz salt and loaded onto a quartz frit at the center of a quartz-tube microreactor, which was heated inside an electric furnace. All samples were used without activation. The gases used were helium (grade 5.0), 10% CO/He or 50% CO/He, 50% CO_2/He or pure CO_2 (grade 4.0), and 50% H_2/He or pure H_2 (ultrahigh purity). All gas mixtures were certified calibration gases. A hydrocarbon trap was

Table 1. Physical Properties of Catalyst Samples[a]

sample	atomic composition (%) measured by ICP: Cu/(Cu + Ce + La) or Fe/(Fe + Ce + La)	atomic composition (%) measured by ICP: La/(La + Ce) or Zr/(Zr + Ce)	BET surface area (m^2/g)	XRD: crystalline phase	XRD: CeO_2 particle size[b](nm)	XRD: CeO_2 lattice constant[c] (Å)
Ce(8% La)O_x	–	7.12	98	CeO_2[13]	7.1[10]	NM[d]
5% Cu–Ce(8% La)O_x	5.21	7.45	107	CeO_2[13]	5.2[10]	NM
10% Cu–Ce(8% La)O_x	10.2	7.55	112	CeO_2	5.1	5.44
10% Cu–Ce(8% La)O_x used[e]	–	–	NM	CeO_2	6.0	5.44
15% Cu–Ce(8% La)O_x	15.5	7.64	85	CeO_2, CuO[13]	NM	NM
40% Cu–Ce(8% La)O_x	41.7	7.93	66	CeO_2, CuO[13]	NM	NM
6.2% Fe–Ce(8% La)O_x	6.71	7.87	109	NM	NM	NM
13% Fe–Ce(8% La)O_x	12.6	7.57	98	CeO_2	5.2	5.42
29% Fe–Ce(8% La)O_x	28.4	8.31	80	NM	NM	NM
Ce(30% La)O_x	–	28.8	103	CeO_2, La_2CO_5	4.7	5.45
Ce(30% La)O_x used[f]	–	–	72	CeO_2, La_2CO_5	5.0	5.45
10% Cu–Ce(30% La)O_x	9.4	28.6	81	CeO_2, La_2CO_5	5.1	5.44
10% Cu–Ce(30% La)O_x used[g]	–	–	65	CeO_2, La_2CO_5	5.8	5.44
10% Cu–Ce(24% Zr)O_x	10.2	24.2	92	CeO_2	5.0	5.36
10% Cu–Ce(24% Zr)O_x used[f]	–	–	74	CeO_2	5.3	5.35
C12-4-02[h]	–	–	96	NM	–	–

[a] All catalysts except C12-4-02 were prepared by the UGC method; calcined in air at 650 °C, 4 h. [b] Calculated on the basis of the peak width of crystal plane (111), using the Scherrer equation. [c] Average of values calculated from crystal planes (111), (200), (220), (311), and (222) using Bragg's law. [d] NM = not measured. [e] Used in 10% CO–34% H_2O–10% CO_2–15% H_2–He at 300–600 °C with a 50 °C interval, then 400 °C, 1.5 h at each temperature. [f] Used in 11% CO–23% H_2O–11% CO_2–17% H_2–He at 450°C, 20 h. [g] Used in 11% CO–23% H_2O–11% CO_2–17% H_2–He at 450°C, 32 h. [h] 80–95 wt % Fe_2O_3, 5–10 wt % Cr_2O_3, <5 wt % CrO_3, 1–5 wt % CuO, 1–5 wt % graphite; supplied by United Catalysts, Inc., and tested after crushing to <150-μm-size particles

connected at the outlet of the CO/He gas cylinder to remove any iron carbonyl from the CO/He mixture. Water was injected into the flowing gas stream by a calibrated syringe pump and was vaporized in the heated gas feed line before entering the reactor. A condenser filled with ice was installed at the reactor exit to collect water. The exit gas was analyzed with a Hewlett-Packard 5890A gas chromatograph, equipped with a thermal conductivity detector and a $^1/_4$-in.-diameter × 6-ft-long Carbosphere column for CO and CO_2 separation. The CO conversion was calculated from the concentrations of CO and CO_2 detected. No methane formation occurred, even when H_2 and CO_2 were included in the feed gas mixture.

Activation energies were calculated from the reaction rates at CO conversions of <20%. The reaction rate was calculated according to the expression

$$\text{rate} = N_{CO}X_{CO}/W_{cat}\,(\text{mol g}^{-1}\,\text{s}^{-1}) \qquad (1)$$

where N_{CO} is the molar flow rate of CO in the feed gas in moles per second, X_{CO} is the percentage conversion of CO to CO_2, and W_{cat} is the catalyst weight in grams.

Results and Discussion

Table 1 lists the bulk compositions, BET surface areas, ceria crystallite sizes, and ceria lattice constants of the catalyst samples prepared and tested in this work. The compositions in the bulk are almost the same as those in the preparation. The samples containing up to 15 atom % Cu or Fe, after calcination at 650 °C, have surface areas of around 90 m^2/g. At higher than 15 atom % content, addition of Cu or Fe decreases the surface area of the La-doped ceria.

It has been reported by Li et al.[13] that, in the copper–ceria system, Cu or CuO nanoparticles cannot be detected by XRD up to ~15 atom % copper content. Similarly, we did not see reflections of Cu compounds in all of the samples listed in Table 1. Particles of Fe or its oxides in our iron–ceria catalysts are also too small to be detected by XRD. In the Zr-doped samples and the 8 atom % La-doped samples, there was no reflection of lanthana or zirconia because both of these oxides go into solid solution with ceria, and the only XRD-detectable phase was ceria. In the samples with 30 atom % La, small amounts of hexagonal, tetragonal, and monoclinic crystals of lanthanum oxide carbonate (La_2CO_5) were identified in addition to ceria (Table 1); only hexagonal La_2CO_5 still existed after use of the catalyst in the WGS reaction. The lattice parameter of ceria (5.41 Å) increases with La^{3+} doping and decreases with Zr^{4+} doping, as a result of the difference in the ionic radii ($La^{3+} > Ce^{4+} > Zr^{4+}$).

Used samples (either 32 or 20 h) lost about 20% of their surface area (Table 1). Concomitantly, the crystal size of ceria increased by about 20% as measured by XRD.

Cu- or Fe–Ce(8% La)O_x catalysts (with different contents of Cu or Fe) were screened in a 2% CO–10% H_2O–He gas mixture. The catalyst amount was 0.15 g, and the contact time was 0.09 g s cm^{-3}. The space velocity (SV) was 80 000 h^{-1} (NTP), except for the commercial iron–chrome catalyst, C12-4-02 (48 000 h^{-1}), because of its different density. Steady-state CO conversion plots are shown in Figure 1. The Fe–Ce(8% La)O_x samples have higher activities than Ce(8% La)-O_x, indicating that addition of Fe increases the activity of ceria. The commercial catalyst C12-4-02 is more active than the Fe–Ce(8% La)O_x samples, but all of the Cu–Ce(8% La)O_x samples are much more active than C12-4-02. The CuO contained in C12-4-02 might be the reason that C12-4-02 is more active than the Fe–Ce-(8% La)O_x samples. Among the copper–ceria samples, 10% Cu–Ce(8% La)O_x and 15% Cu–Ce(8% La)O_x were the most active. The 13% Fe–Ce(8% La)O_x was the most active among the iron–ceria samples.[22]

H_2 TPR data for various catalyst compositions are presented in Figures 2 and 3 and Table 2. These results help us understand the differences in WGS activity among the catalysts shown in Figure 1. The low-temperature peak (surface oxygen reduction) of ceria

Table 2. H_2 TPR Peak[a] Temperatures and Areas (H_2 Consumption)

sample	temperature (°C)	H_2 consumption: total (mmol of H_2/g)	H_2 consumption: by ceria only[b] (mol of H_2/mol of CeO_2)
C8L[c]	408	0.560	0.106
1% Cu−C8L	135, 320	0.539	0.092
5% Cu−C8L	126, 132, 145 (small)	0.737	0.085
10% Cu−C8L	96, 103, 129 (small), 164 (small)	1.156	0.108
40% Cu−C8L	94, 154 (shoulder), 195	3.414	0.078
6.2% Fe−C8L	123, 367		
13% Fe−C8L	119, 359		
29% Fe−C8L	362		

[a] Peaks below 500 °C. [b] After subtraction of the H_2 consumed by CuO. [c] Ce(8% La)O_X is denoted as C8L.

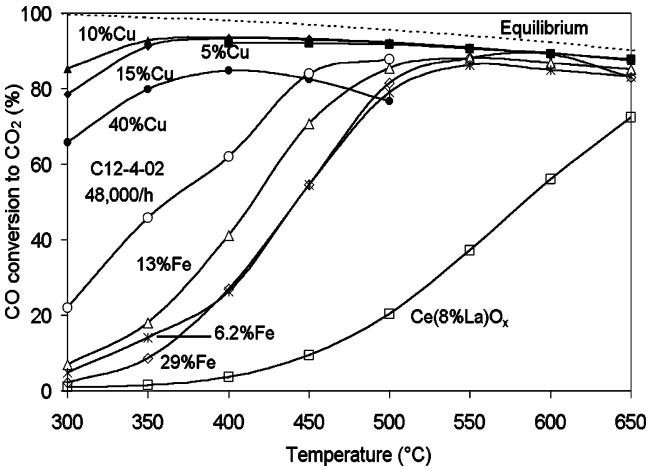

Figure 1. Steady-state WGS performance of Cu− and Fe−Ce-(8% La)O_x in 2% CO−10% H_2O−He, 0.09 g s cm^{-3}, SV = 80 000 h^{-1} (except C12-4-02).

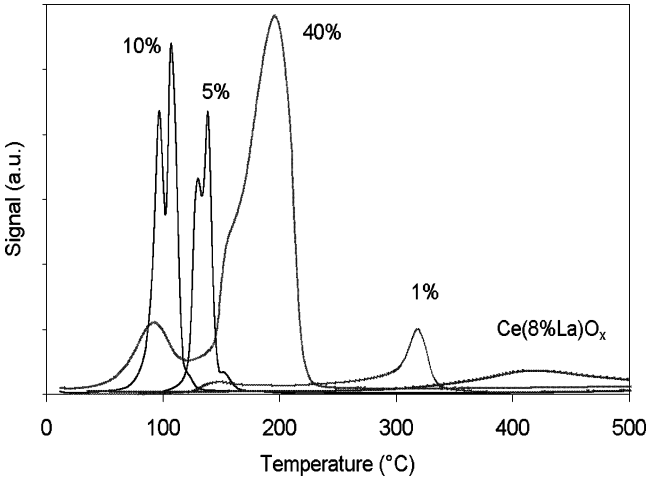

Figure 2. H_2 TPR of *x*% Cu−Ce(8% La)O_x samples.

shifts to lower temperatures upon addition of Cu. As shown in Figure 2, the presence of even 1 atom % Cu shifts the peak reduction temperature by more than 100 °C. With higher copper contents, the effect is much more pronounced. Thus, Cu dramatically increases the reducibility of ceria, as has been amply documented in the literature.[13,17,23] As shown in Table 2, the normalized hydrogen consumption does not change much with addition of copper above ∼1 atom %. There is no need to use ceria catalysts containing more than ∼10 atom % copper, in agreement with the activity data of Figure 1. Figure 1 shows that the sample containing 40 atom % Cu was inferior, probably because of the lower surface area and further sintering during reaction. Addition of Fe increases the reducibility of ceria but to a lesser

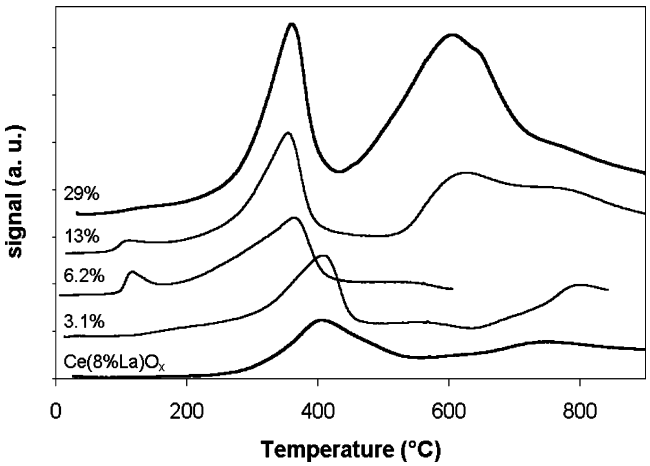

Figure 3. H_2 TPR of *x*% Fe−Ce(8% La)O_x samples.

extent than Cu, as shown in Figure 3 and Table 2. Promotion of iron-based shift catalysts by ceria has been reported in the literature and attributed to enhancement of reducibility.[19,20] The activity tests of the iron oxide−ceria catalysts performed in the present work correlate well with the H_2 TPR results of Figure 3. The best iron−ceria catalyst shown in Figure 1 was the one containing 13 atom % Fe. Interestingly, as shown in Figure 3, for the sample containing 13 atom % Fe, the iron oxide reduction begins and peaks at lower temperatures. The reduction of the bulk oxygen of ceria is not affected by the presence of either iron (Figure 3) or copper oxide (not included in Figure 2).

In many practical cases, hydrogen is obtained from coal gasification. As mentioned above, CO_2 enrichment of the gas occurs when the WGS reaction is integrated with hydrogen permeation through a dense membrane. Therefore, the WGS activities of the 10% Cu−Ce(8% La)O_x and 13% Fe−Ce(8% La)O_x catalysts were tested and compared with that of the commercial catalyst C12-4-02 in a simulated coal gas mixture with a molar composition 10% CO−34% H_2O−10% CO_2−15% H_2−He (here helium is used instead of N_2) and in a CO_2-rich gas containing 2% CO−10% H_2O−35% CO_2−He, both at a contact time of 0.09 g s cm^{-3}. In both gas mixtures (Figures 4 and 5), the ranking of the catalysts is the same as that in Figure 1, i.e., the 10% Cu−Ce(8% La)-O_x is more active than C12-4-02, which is superior to 13% Fe−Ce(8% La)O_x. Lund et al. [6] have reported a dramatic poisoning effect of CO_2 on iron oxide-based catalysts, whereby the reaction rate decreased by several orders of magnitude in CO_2-rich gas. Copper−ceria, on the other hand, exhibits very good activity, reaching equilibrium CO conversions above 450 °C in the simulated coal gas mixture and at high space velocity (80 000 h^{-1}, NTP, Figure 4). After all the measurements from

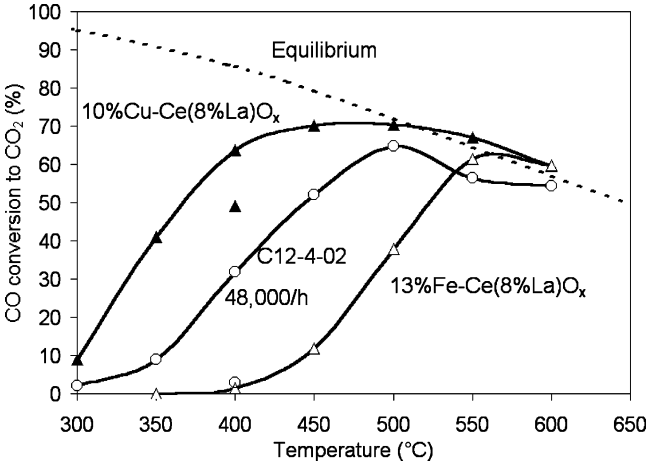

Figure 4. Steady-state WGS activity in a simulated coal gas composition, 10% CO−34% H_2O−10% CO_2−15% H_2−He, 0.09 g s cm^{-3}, SV = 80 000 h^{-1} (except C12-4-02). Single filled triangle, conversion at 400 °C after the 300−600 °C measurement over 10% Cu−Ce(8% La)O_x; single circle, conversion at 400 °C after the 300−600 °C measurement over C12-4-02.

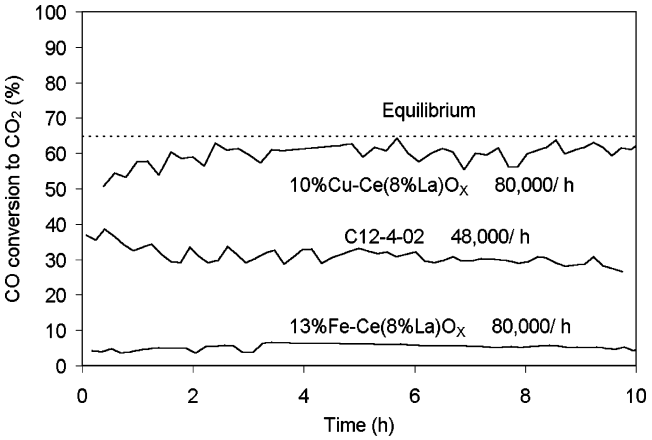

Figure 5. Catalyst activity/stability in 2% CO−10% H_2O−35% CO_2−He, 450 °C, 0.09 g s cm^{-3}, SV = 80 000 h^{-1} (except C12-4-02).

300 to 600 °C (50 °C intervals, 1.5 h at each temperature), the CO conversions over both 10% Cu−Ce(8% La)-O_x and C12-4-02 were checked again at 400 °C, as shown by the single filled triangle and the single circle, respectively, in Figure 4. The CO conversions over both catalysts dropped, but both were still higher than that over the 13% Fe−Ce(8% La)O_x sample at 400 °C before exposure to high temperatures; the conversion over 10% Cu−Ce(8% La)O_x was still higher than that over C12-4-02. The activity of copper−ceria is stable in the gas mixture with the artificially high CO_2 content (Figure 5). Thus, this type of catalyst has merits for the high-temperature shift reaction carried out in a membrane reactor.

Effect of Dopant. Steady-state conversions of CO in the WGS reaction over the 10% Cu−Ce(dopant)O_x samples with dopants 8% La, 30% La, and 24% Zr were measured in the microreactor in a gas mixture of 10% CO−30% H_2O−10% CO_2−15% H_2−He, with a catalyst amount of 0.05 g and at a contact time 0.012 g s cm^{-3}. The activities were in the order 30% La > 24% Zr > 8% La. Because the surface areas of these samples are all similar (Table 1), we conclude that the effect is chemical and not scalable with the surface area.

Figure 6 shows the stabilities of 10% Cu−Ce(30% La)O_x and 10% Cu−Ce(24% Zr)O_x with time on stream

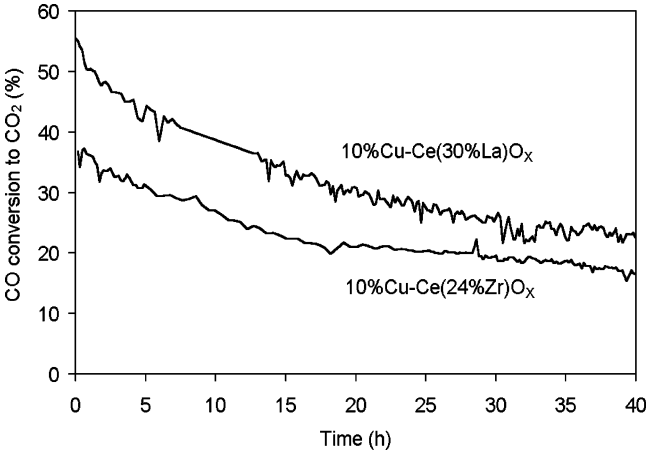

Figure 6. Stability of 10% Cu−Ce(30% La)O_x and 10% Cu−Ce-(24% Zr)O_x in 11% CO−23% H_2O−11% CO_2−17% H_2−He, 0.0303 g s cm^{-3}, 450 °C.

Table 3. XPS Analysis of 10% Cu−Ce(30% La)O_x

atomic metal ratio	before reaction	after reaction[a]
Cu/(Cu + Ce + La)	0.133	0.208
La/(Ce + La)	0.330	0.340

[a] Used in 10% CO−30% H_2O−10% CO_2−15% H_2−He at 450 °C for 34 h.

at 450 °C. The contact time was 0.0303 g s cm^{-3}. Higher conversions of CO were measured over the La-doped sample throughout the 40-h-long test period. Both catalysts lost some activity rapidly at the beginning, but their activities became stable after 20 h on stream. No carbon deposition was found on either of the two used samples, as checked by temperature-programmed oxidation (TPO). The BET surface areas of both catalysts decreased by about 20% after use for either 32 or 20 h (Table 1), and the increase in ceria crystal size of both samples (Table 1) was also around 20%. The drop of CO conversion over both catalysts (after 32 or 20 h) was more than 20%. Over both catalysts, the CO conversion after 2 h was around 1.6 times the conversion after 20 h. Therefore, the loss of surface area (together with the increase in ceria crystal size) was not the only reason for the observed activity loss. XPS analysis of the 10% Cu−Ce(30% La)O_x sample (Table 3) showed that, after reaction under similar conditions (10% CO−30% H_2O−10% CO_2−15% H_2, 450 °C, 34 h), Cu enrichment of the surface from 13 to 21 atom % took place, whereas the surface concentration of La did not change. It is possible that copper enrichment of the ceria surface contributed to the activity loss.

Rate Measurements. The WGS reaction rate was measured over 10% Cu−Ce(30% La)O_x catalyst in the simulated coal gas mixture used in Figure 6. The apparent activation energy of the reaction was calculated from the following equations

$$\text{rate} = R_f(1 - \beta) \tag{2}$$

$$R_f = R_{f0} \exp(-E_a/RT) \tag{3}$$

where β is the approach to equilibrium

$$\beta = P_{CO_2}P_{H_2}/(K_{eq}P_{CO}P_{H_2O}) \tag{4}$$

R_f is the forward reaction rate, K_{eq} is the WGS reaction

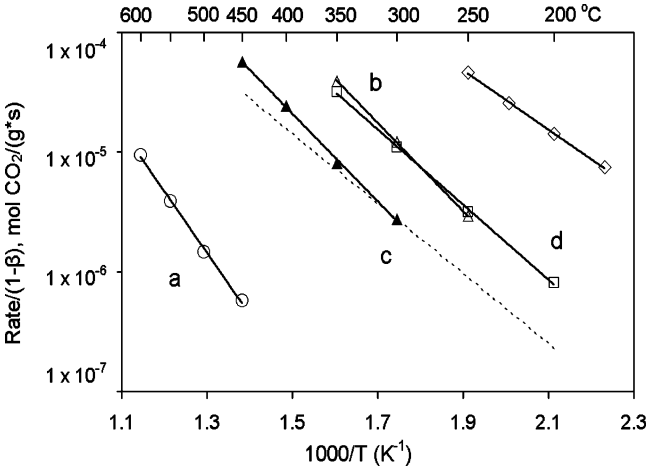

Figure 7. Steady-state WGS reaction rates over 10% Cu−Ce(30% La)O_x and Ce(30% La)O_x in 11% CO−23% H_2O−11% CO_2−17% H_2−He and comparison with other catalysts. $\beta = P_{CO_2}P_{H_2}/(K_{eq}P_{CO}P_{H_2O})$. (a) Ce(30% La)$O_x$, E_a = 98.5 kJ/mol; (b, △) 10% Cu−Ce(30% La)O_x, E_a = 70.6 kJ/mol; (c) 10% Cu−Ce(30% La)O_x used at 450 °C for 20 h, E_a = 70.2 kJ/mol; (d, □) 10% Cu−Ce(8% La)O_x (calcined at 400 °C, surface area = 200 m^2/g) in 11% CO−26% H_2O−7% CO_2−26% H_2−He, data from ref 12, E_a = 60 kJ/mol; (e, ◇) G-66A (supplied by United Catalysts, Inc., 42 wt % CuO, 47 wt % ZnO, 10 wt %Al_2O_3, surface area = 49 m^2/g,), 11% CO−26% H_2O−7% CO_2−26% H_2−He, data from ref 12, E_a = 47 kJ/mol; (dashed line) 8 wt % copper−ceria, extrapolated to 11% CO−23% H_2O−11% CO_2−17% H_2−balance inert using the reaction orders, activation energy, and rate at 200 °C in 7% CO−22% H_2O−8.5% CO_2−37% H_2−balance inert as reported in ref 14.

equilibrium constant, E_a is the apparent activation energy in joules per mole, R = 8.314 J mol^{-1} K^{-1} is the ideal gas constant, and T is temperature in Kelvin. The factor $(1 - \beta)$ represents the effect of the reverse reaction. If the feed gas does not include CO_2 and H_2, $\beta = 0$, and eq 3 is used to calculate the activation energy.

Figure 7 shows Arrhenius-type plots for the WGS reaction rates measured over the 10% Cu−Ce(30% La)O_x and the copper-free Ce(30% La)O_x catalysts. The apparent activation energy of the reaction over these catalysts is 70.4 and 98.5 kJ/mol, respectively. This large difference is attributed to the modification of the surface of ceria by the addition of copper. As discussed before, copper greatly increases the reducibility of the surface oxygen of ceria. This modified site is the active site for the WGS reaction. The reaction pathway on copper-free ceria is different and has a larger activation energy.

At high temperatures, such as 450 °C, the fresh 10% Cu−Ce(30% La)O_x sample deactivates rapidly in the initial time on stream (Figure 6). To obtain a stable conversion and reaction rate and an accurate measurement of the activation energy, we measured the reaction rate over the 10% Cu−Ce(30% La)O_x sample after it had been used in the reaction gas mixture at 450 °C for 20 h. The same activation energy was measured over the used sample (from 300 to 450 °C) and the fresh one (from 250 to 350 °C). The Ce(30% La)O_x catalyst does not deactivate that rapidly, so the fresh sample was used in all tests.

A comparison of reaction rates with other copper−ceria catalysts[12,14] is also shown in Figure 7. The values of reaction rate on the 10% Cu−Ce(8% La)O_x catalyst prepared by the same UGC procedure but calcined at 400 °C and tested in a slightly different gas composition[12] are very close to the rates reported here. If extrapolated to our gas composition, the rates in ref 12 would drop slightly and cross ours as 250 °C. The difference in activation energy is not large and might be due to the different gas compositions used. Another comparison was made with the rates on an 8 wt % copper−ceria sample, reported recently by Koryabkina et al.[14] This is shown by a dashed line in Figure 7, calculated using the reported reaction orders, activation energy, and rate at 200 °C in 7% CO−22% H_2O−8.5% CO_2−37% H_2−balance inert gas. Although not exposed to high temperatures, this copper−ceria sample is comparable to our 450 °C used sample but less active than our fresh copper−ceria catalyst, which contains only ∼5 wt % Cu. A possible explanation for the higher activity of our sample is the presence of lanthana and the different preparation method, which leads to better dispersion of Cu in ceria.

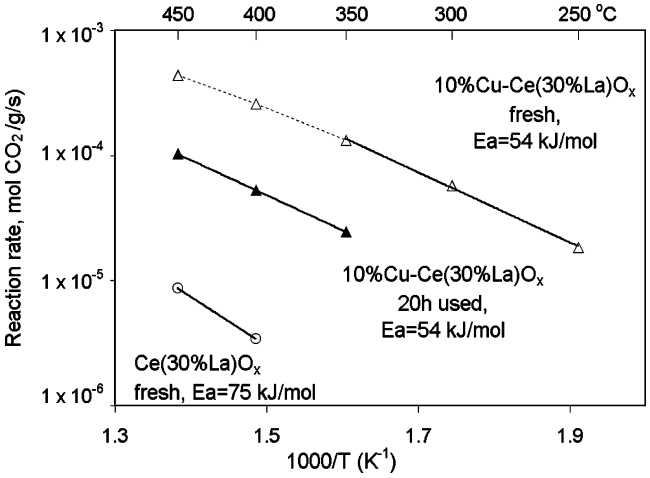

Figure 8. Steady-state WGS reaction rates over 10% Cu−Ce(30% La)O_x and Ce(30% La)O_x in 11% CO−23% H_2O−He.

Figure 8 shows WGS reaction rates measured over the 10% Cu−Ce(30% La)O_x and Ce(30% La)O_x samples in a gas mixture free of H_2 and CO_2: 11% CO−23% H_2O−He. Under these conditions, both samples showed better stability than in the product-containing gas. The fresh 10% Cu−Ce(30% La)O_x sample was first tested at 450 °C for 1 h and then at the temperatures 400, 350, 300, and 250 °C for 40 min each. After the catalyst had been tested for 20 h at 450 °C, the activation energy did not change. The apparent activation energy is 54 kJ/mol over 10% Cu−Ce(30% La)O_x and 75 kJ/mol over Ce(30% La)O_x, i.e., considerably lower than the values measured in the simulated coal gas mixture in Figure 7, and the reaction rates were higher than those in Figure 7. Therefore, inhibition of the reaction by at least one of the two reaction products (H_2 or CO_2) occurs, but the total inhibitory effect of H_2 and CO_2 decreases with temperature.

The WGS reaction orders in CO, H_2O, CO_2, and H_2 were evaluated at 450 °C (Figure 9). The catalyst sample was pretreated in 10% CO−30% H_2O−He at 450 °C for 30 h to avoid deactivation during the kinetics measurements. The rate data were fitted with a power-law equation of the form

$$\text{rate} = k_f P_{CO}{}^a P_{H_2O}{}^b P_{CO_2}{}^c P_{H_2}{}^d (1 - \beta) \qquad (5)$$

where the rate is in moles per gram per second; P_i, in atmospheres, is the partial pressure of component i; k_f is the forward reaction rate constant; a−d are the forward reaction orders; and β is the approach to equilibrium as described by eq 4.

Table 4. Comparison of Reaction Orders and Apparent Activation Energies

catalyst	ref	activation energy, E_a (kJ/mol)	temp[a] (°C)	reaction orders (and range) CO	H_2O	CO_2	H_2
10 atom % Cu−Ce(30 atom % La)O_x[b]	this work	70.4	450	0.8 1−10%	0.2 11−50%	−0.3 5−35%	−0.3 5−40%
8 wt % CuO−CeO_2[c]	14	56	240	0.9 5−25%	0.4 10−46%	−0.6 5−30%	−0.6 25−60%
10 atom % Cu−Ce(8 atom % La)O_x[d,e]	12	60	300	0.8 3.4−25%	0.5 2.7−16%	−0.5 13−44%	−0.4 13−44%
Fe_2O_3−Cr_2O_3	1	−		0.9	0.25	−0.6	0
promoted Fe_2O_3−Cr_2O_3	2	95	300−350	1.1	0.53	0	0

[a] Temperature at which the reaction rates were measured. [b] Varying CO, H_2O, CO_2 or H_2 in 10% CO−30% H_2O−10% CO_2−15% H_2−balance He. [c] Varying CO, H_2O, CO_2 or H_2 in 7% CO−22% H_2O−8.5% CO_2−37% H_2−balance Ar. [d] Varying CO, H_2O, CO_2 or H_2 in 11% CO−26% H_2O−7% CO_2−26% H_2−balance He. [e] Prepared by the UGC method, calcined at 400 °C.

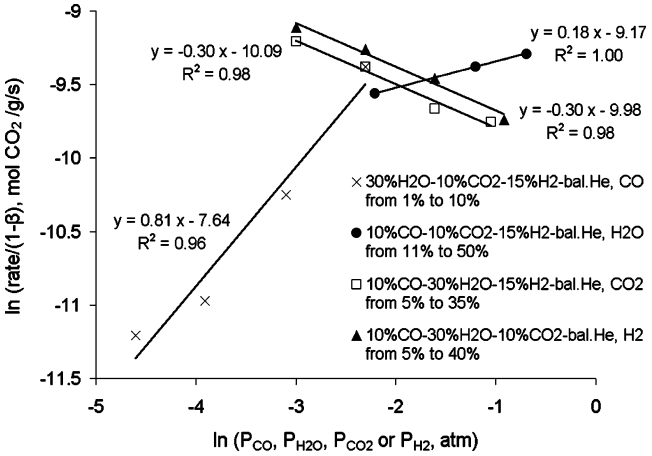

Figure 9. Effects of CO, H_2O, CO_2, and H_2 on WGS rates over 10% Cu−Ce(30% La)O_x (30 h used in 10% CO−30% H_2O−He); 450 °C; 10% CO−30% H_2O−10% CO_2−15% H_2−He; varying CO from 1 to 10%, H_2O from 11 to 50%, CO_2 from 5 to 35%, or H_2 from 5 to 40%; $\beta = P_{CO_2}P_{H_2}/(K_{eq}P_{CO_2}P_{H_2O})$.

The reaction orders in CO, H_2O, CO_2, and H_2 were found to be 0.8, 0.2, −0.3, and −0.3, respectively. This shows that H_2O has very little effect on the reaction rate and that both CO_2 and H_2 weakly inhibit the reaction.

A comparison of reaction orders and apparent activation energies with those over other catalysts[1,2,12,14] is presented in Table 4. The gas composition used in our work was not significantly different from that of Koryabkina et al.[14] Compared to their data over copper−ceria, the reaction order in CO over our catalyst is similar, but the order in H_2O is lower, and the inhibition by either CO_2 or H_2 is less. We attribute these differences to the difference in temperature; our tests were run at 450 °C, a temperature much higher than the 240 °C examined in ref 14.

The almost first-order dependence of the WGS reaction rate on P_{CO} and almost zeroth-order dependence on P_{H_2O} are interesting and indicative of a surface saturated with hydroxyls. Whether CO adsorbs on neutral or charged copper clusters or copper ions embedded in the ceria lattice is of fundamental interest and will be explored in future work. The important finding is that the Cu−O−Ce species are stable under WGS conditions at 450 °C. Thus, this catalyst is a good alternative to the iron−chrome catalyst for any WGS application, and it is currently the only choice for membrane reactor applications.

Conclusions

In this work, we have demonstrated that copper−ceria is an excellent HTS catalyst, not suffering from the severe instability of iron−chrome catalysts in CO_2-rich gases. Ceria participates in the WGS reaction; its surface properties are crucial for high activity. The kinetics of the WGS reaction over 10% Cu−Ce(30% La)-O_x were measured over the temperature range 300−450 °C. A strong dependence on CO and a weak dependence on H_2O were found at 450 °C, and inhibition by the reaction products was weak. No carbon deposition took place on the catalysts under these conditions. Catalysts lost some activity in the initial time on stream but were stabilized thereafter. Thus, cerium oxide stabilizes copper in active form under WGS conditions at temperatures as high as 450 °C.

Acknowledgment

This work was supported by the U.S. Department of Energy, University Coal Research Program, Grant DE-FG2600-NT40819.

Literature Cited

(1) Newsome, D. S. The Water−Gas Shift Reaction. *Catal. Rev.-Sci. Eng.* **1980**, *21*, 275.

(2) Keiski, R. L.; Salmi, T.; Niemistö, P.; Ainassaari, J.; Pohjola, V. J. Stationary and Transient Kinetics of the High-Temperature Water−Gas Shift Reaction. *Appl. Catal. A* **1996**, *137*, 349.

(3) Rhodes, C.; Hutchings, G. J.; Ward, A. M. Water−Gas Shift Reaction: Finding the Mechanistic Boundary. *Catal. Today* **1995**, *23*, 43.

(4) Lund C. R. F. Effect of Adding Co to MoS_2/Al_2O_3 upon the Kinetics of the Water−Gas Shift. *Ind. Eng. Chem. Res.* **1996**, *35*, 3067.

(5) Flytzani-Stephanopoulos, M.; Meldon, J.; Qi, X. *Water Gas Shift with Integrated Hydrogen Separation Process*; Annual Report to the U.S. Department of Energy; Grant DE-FG2600-NT40819; Dec 2002.

(6) Lund C. R. F. *Water Gas Shift Kinetics over Iron Oxide Catalysts at Membrane Reactor Conditions*; Final Report to the U.S. Department of Energy; Grant DE-FG26-99FT40590; Aug 2002.

(7) Bunluesin, T.; Gorte, R. J.; Graham, G. W. Studies of the Water−Gas-Shift Reaction on Ceria-Supported Pt, Pd, and Rh: Implications for Oxygen-Storage Properties. *Appl. Catal. B* **1998**, *15*, 107.

(8) Wang, X.; Gorte, R. J.; Wagner J. P. Deactivation Mechanisms for Pd/Ceria during the Water−Gas-Shift Reaction. *J. Catal.* **2002**, *212*, 225.

(9) Fu, Q.; Weber, A.; Flytzani-Stephanopoulos, M. Nanostructured Au−CeO_2 Catalyst for Low-Temperature Water−Gas Shift. *Catal. Lett.* **2001**, *77*, 87.

(10) Fu, Q.; Kudriavtseva, S.; Saltsburg, H.; Flytzani-Stephanopoulos, M. Gold−Ceria Catalysts for Low-Temperature Water−Gas Shift Reaction. *Chem. Eng. J.* **2003**, *93*, 41.

(11) Fu, Q.; Saltsburg, H.; Flytzani-Stephanopoulos, M. Active Nonmetallic Au and Pt Species on Ceria-Based Water−Gas Shift Catalysts. *Science* **2003**, *301*, 935; published online July 3, 2003; 10.1126/science.1085721.

(12) Fu, Q. Activity and Stability of Nanostructured Gold−Cerium Oxide Catalysts for the Water−Gas Shift Reaction. Ph.D. Thesis, Tufts University, Medford, MA, 2004.

(13) Li, Y.; Fu, Q.; Flytzani-Stephanopoulos, M. Low-Temperature Water−Gas Shift Reaction over Cu- and Ni-Loaded Cerium Oxide Catalysts. *Appl. Catal. B* **2000**, *27*, 179.

(14) Koryabkina, N. A.; Phatak, A. A.; Ruettinger, W. F.; Farrauto, R. J.; Ribeiro, F. H. Determination of Kinetic Parameters for the Water−Gas Shift Reaction on Copper Catalysts under Realistic Conditions for Fuel Cell Applications. *J. Catal.* **2003**, *217*, 233.

(15) Padeste, C.; Cant N. W.; Trimm, D. L. The Influence of Water on the Reduction and Reoxidation of Ceria. *Catal. Lett.* **1993**, *18*, 305.

(16) Trovarelli, A. Catalytic Properties of Ceria and CeO_2-Containing Materials. *Catal. Rev.-Sci. Eng.* **1996**, *38*, 439.

(17) Kundakovic, L.; Flytzani-Stephanopoulos, M. Reduction Characteristics of Copper Oxide in Cerium and Zirconium Oxide Systems. *Appl. Catal. A* **1998**, *171*, 13.

(18) Ladebeck, J.; Kochloefl, K. Cr-Free Iron Catalysts for Water−Gas Shift Reaction. *Stud. Surf. Sci. Catal.* **1995**, *91*, 1079.

(19) Ou, X.; Cheng, J.; Wang H.; Xiao, Y. Effects of Metal Oxides on Stability and Activity of Iron-Based Chromia-Free Catalysts for Water−Gas Shift Reaction. *J. Nat. Gas Chem.* **1999**, *8*, 231.

(20) Hu, Y.; Jin, H.; Liu, J.; Hao, D. Reactive Behaviors of Iron-Based Shift Catalyst Promoted by Ceria. *Chem. Eng. J. (Lausanne)* **2000**, *78*, 147.

(21) West, A. R. *Solid State Chemistry and Its Applications*; John Wiley & Sons: New York, 1995.

(22) Flytzani-Stephanopoulos, M.; Meldon, J.; Qi, X.; *Water Gas Shift with Integrated Hydrogen Separation Process*; Annual Report to the U.S. Department of Energy; Grant DE-FG2600-NT40819; Dec 2001.

(23) Liu, W.; Flytzani-Stephanopoulos, M. Transition Metal-Promoted Oxidation Catalysis by Fluorite Oxides: A Study of CO Oxidation over Cu−CeO_2. *Chem. Eng. J.* **1996**, *64*, 283.

Received for review July 22, 2003
Revised manuscript received February 13, 2004
Accepted February 16, 2004

IE0306170